ANALYSIS OF THE ELASTIC-PLASTIC PROBLEMS BY THE MATRIX DISPLACEMENT METHOD

Y. Yamada*, T. Kawai** and N. Yoshimura***
The Institute of Industrial Science
The University of Tokyo, Tokyo, Japan

and T. Sakurai****
Mitsubishi Atomic Power Industries, Inc.
Tokyo, Japan

An unified treatment on the matrix methods of analysis of the elastic-plastic problems will be described in this paper. In the earlier section the stress-strain matrices suitable for analyzing the elastic-plastic problems are derived first based on the Mises yield condition and its associated flow rule which is the Prandtl-Reuss equation. Examples of the stress-strain matrices will be shown as applied to the plane problems, the axisymmetric as well as Saint-Venant torsion problems. As numerical examples for the plane and axisymmetric problems, tensile test of a sheet and a round bar with V notches will be treated. As for Saint-Venant torsion problems, a new displacement method of solution will be proposed as an alternative of the existing matrix method of solution based on the well known stress function. The elastic-plastic torsion problems can be treated in comparatively easy manner by the proposed displacement method. The present paper includes, in the last section, the discussion of the elastic-plastic analysis of the frame structures. Although the application of the matrix methods to the elastic-plastic frame analysis is not necessarily new, attempt will be made to establish an unified procedure for the solution of relevant problems, giving considerations to (1) the relation to the continuum problems, and (2) treatment of load distributed along the span. Through the present study, it is concluded that the plastic limit design will be replaced, in the near future, by the matrix methods which are ideally suited for the analysis of nonlinear problems involving plastic deformation.

---

*Professor
**Associate Professor
***Assistant
****Research Engineer

SECTION I

INTRODUCTION

It has been considered for long time that the elastic-plastic problem is extremely intractable in the continuum mechanics. Although the importance of plasticity solution has been recognized in the earlier days in the field of material science, 'intractableness' has been fatal defect and also has made the theory of plasticity inaccessible. So, the development of the very ingenious method of solution called as the plastic limit analysis may be considered the very last countermeasure to avoid difficulties in the analysis of the elastic-plastic problems. It may be said that recent development of matrix methods has completely changed the situation.

In the stage of application where the iterative solution of plasticity problems was sought on the basis of the total strain, or deformation theory of plasticity, matrix methods were not considered to be so powerful for analysis of nonlinear problems. The recent success in application of matrix methods to plasticity problems could be mainly attributed to their bridging to the incremental theory of plasticity. In the earlier days of 1950 --- when development of matrix methods had been just started with evolution of the electronic digital computers --- the incremental theory had been established by the scientists and engineers in plasticity such as Hill (Reference 1) and others. As well the introduction of the finite element method in the field of structural and continuum mechanics, the establishment of the incremental approach in the field of plasticity theory should be highly evaluated.

The Prandtl-Reuss equation has been widely accepted as the basis of the incremental theory of plasticity. Not only is the Prandtl-Reuss equation generally consistent with experimental observations, but it is quite fortunate that the equation is ideally suited for theoretical analysis by means of digital computers. As is well known, the Prandtl-Reuss equation is derived from the Mises yield condition as the plastic potential. In the earlier part of this paper, the stress-strain matrix written in the convenient form for its application to the matrix displacement method will be derived through the inversion of the Prandtl-Reuss equation, and various forms of the matrix will be given for specific cases such as the plane stress, plane strain and axisymmetric problems.

Once the stress-strain matrix has been formulated (the possible extension of the present approach to the soil and rock mechanics would be obvious), the elastic-plastic problems can be

solved by using the standard procedure of analysis well established in the matrix displacement method, except simple modification of the stress-strain matrices (from elastic to plastic) for yielded discrete elements. Thus, we can determine the elastic-plastic boundary with the growth of plastic region in continua, while in case of frame structures we can trace all the process of plastic hinge formation up to the plastic collapse of the structures.

In the process of such elastic-plastic analysis, the yield criteria will be applied for the discrimination of plastic elements (or members) from elastic ones. In the earlier section where analysis of continua is described, a step by step method of tracing the yielding of individual discrete elements will be discussed. In the frame structures, a similar procedure will be applied for consecutive pursuit of the plastic hinge formation at the member-ends or somewhere in the structures.

It must be emphasized that the effects of strain-hardening of the material can be easily taken into account in the elastic-plastic analysis based on the matrix displacement method. Furthermore, the effects of the change of structural configuration due to large displacement as well as the effects of axial forces in the frame structures (more generally, the force-moment interaction in the yield condition) can be allowed for without introducing appreciable difficulty in the matrix methods. Therefore, it can be concluded that the field of application of the methods is extremely broad and the solutions to be obtained are very realistic and significant.

In this paper, general application of the incremental procedure of the matrix displacement method to the elastic-plastic analysis of continuum and frame structures will be discussed, and power of this newly developed technique will be demonstrated by showing, as many as possible, the numeral examples of the following problems: (a) the plane and axisymmetric problems, (b) Saint-Venant torsion, (c) plane trusses and frames.

SECTION II

DERIVATION OF THE PLASTIC STRESS-STRAIN MATRIX

Various matrix methods for the solution of continuum plasticity problems where the material nonlinearity is taken into account are described by Zienkiewicz (Reference 2). Among them the incremental approach seems to be comparatively new and the earlier works of Pope (Reference 3), Marcal and Pilgrim (Reference 4), Marcal and King (Reference 5) and others.

Success of the matrix methods in plasticity problems entirely depends upon the possibility whether the stress-strain relation in plastic range can be postulated in such a form that it may be suitable for application to the matrix methods or not. More precisely, in the case of Prandtl-Reuss equation, formulation of the matrix theory will be successful if the proportionality factor $d\lambda$ involved in the following equations can be expressed either by the stress-increments or by the strain-increments. The equations are:

$$\left.\begin{aligned}
d\epsilon_x &= \sigma_x' \, d\lambda + d(\sigma_x - \nu\sigma_y - \nu\sigma_z)/E \\
d\epsilon_y &= \sigma_y' \, d\lambda + d(\sigma_y - \nu\sigma_z - \nu\sigma_x)/E \\
d\epsilon_z &= \sigma_z' \, d\lambda + d(\sigma_z - \nu\sigma_x - \nu\sigma_y)/E \\
d\gamma_{zy} &= 2\tau_{xy} \, d\lambda + d\tau_{xy}/G \\
d\gamma_{yz} &= 2\tau_{yz} \, d\lambda + d\tau_{yz}/G \\
d\gamma_{zx} &= 2\tau_{zx} \, d\lambda + d\tau_{zx}/G
\end{aligned}\right\} \qquad (1)$$

where σ_x', σ_y', σ_z' are the deviatoric stresses, and $d\gamma_{xy}$, $d\gamma_{yz}$, $d\gamma_{zx}$ denote the engineering shearing strain increments; the other notations being considered to be of self-evidence. In the earlier work of Yamada (Reference 6) the factor $d\lambda$ was shown to be expressed by the following equation:

$$d\lambda = \frac{\sigma_x' \, d\epsilon_x + \sigma_y' \, d\epsilon_y + \sigma_z' \, d\epsilon_z + \tau_{xy} \, d\gamma_{xy} + \tau_{yz} \, d\gamma_{yz} + \tau_{zx} \, d\gamma_{zx}}{\frac{2}{3} \, \bar{\sigma}^2 \, (1 + H'/3G)} \qquad (2)$$

Equation 2 may be easily verified through the combined use of the Mises yield condition

$$\sigma_x'^2 + \sigma_y'^2 + \sigma_z'^2 + 2(\tau_{xy}^2 + \tau_{yz}^2 + \tau_{zx}^2) = \frac{2}{3} \bar{\sigma}^2 \qquad (3)$$

with Equation 1, where $\bar{\sigma}$ denotes the equivalent stress, and H' is the slope of equivalent stress ($\bar{\sigma}$)-equivalent strain ($\int d\bar{\epsilon}^p$) relation; i.e. $H' = d\bar{\sigma}/d\bar{\epsilon}^p$. Substituting Equation 2 into Equation 1 and solving for the stress-increments

$$\{d\sigma\} = [D^p]\{d\epsilon\} \tag{4}$$

where

$$\{d\sigma\} = \begin{Bmatrix} d\sigma_x \\ \vdots \\ d\tau_{zx} \end{Bmatrix} \qquad \{d\epsilon\} = \begin{Bmatrix} d\epsilon_x \\ \vdots \\ d\gamma_{zx} \end{Bmatrix}$$

and

$$[D^p] = \frac{E}{1+\nu}\begin{bmatrix} \frac{1-\nu}{1-2\nu} - \frac{\sigma_x'^2}{S} & & & & & & \text{SYM.} \\ \frac{\nu}{1-2\nu} - \frac{\sigma_x'\sigma_y'}{S} & \frac{1-\nu}{1-2\nu} - \frac{\sigma_y'^2}{S} & & & & & \\ \frac{\nu}{1-2\nu} - \frac{\sigma_x'\sigma_z'}{S} & \frac{\nu}{1-2\nu} - \frac{\sigma_y'\sigma_z'}{S} & \frac{1-\nu}{1-2\nu} - \frac{\sigma_z'^2}{S} & & & & \\ -\frac{\sigma_x'\tau_{xy}}{S} & -\frac{\sigma_y'\tau_{xy}}{S} & -\frac{\sigma_z'\tau_{xy}}{S} & \frac{1}{2} - \frac{\tau_{xy}^2}{S} & & & \\ -\frac{\sigma_x'\tau_{yz}}{S} & -\frac{\sigma_y'\tau_{yz}}{S} & -\frac{\sigma_z'\tau_{yz}}{S} & -\frac{\tau_{xy}\tau_{yz}}{S} & \frac{1}{2} - \frac{\tau_{yz}^2}{S} & & \\ -\frac{\sigma_x'\tau_{zx}}{S} & -\frac{\sigma_y'\tau_{zx}}{S} & -\frac{\sigma_z'\tau_{zx}}{S} & -\frac{\tau_{xy}\tau_{zx}}{S} & -\frac{\tau_{yz}\tau_{zx}}{S} & \frac{1}{2} - \frac{\tau_{zx}^2}{S} & \end{bmatrix} \tag{5}$$

S in Equation 5 is identical with the denominator of Equation 2 and expressed by

$$S = \frac{2}{3}\bar{\sigma}^2(1 + H'/3G) \tag{6}$$

Alternatively, Equation 5 can be derived from the fact that the proportionality factor $d\lambda$ can be expressed in terms of stress-increments as follows:

$$d\lambda = \frac{3}{2}\frac{d\bar{\sigma}}{\bar{\sigma}H'} = \frac{9}{4\bar{\sigma}^2H'}(\sigma_x'\, d\sigma_x + \cdots + 2\tau_{zx}\, d\tau_{zx}) \tag{7}$$

Equation 7 is obtained from the definition of $d\lambda$ and the differential form of Equation 3. The plastic stress-strain matrix $[D^p]$ of Equation 5 corresponds to the well-known elastic stress-strain matrix

$$[D^e] = \frac{E}{1+\nu}\begin{bmatrix} \frac{1-\nu}{1-2\nu} & \frac{\nu}{1-2\nu} & \frac{\nu}{1-2\nu} & 0 & 0 & 0 \\ \frac{\nu}{1-2\nu} & \frac{1-\nu}{1-2\nu} & \frac{\nu}{1-2\nu} & 0 & 0 & 0 \\ \frac{\nu}{1-2\nu} & \frac{\nu}{1-2\nu} & \frac{1-\nu}{1-2\nu} & 0 & 0 & 0 \\ 0 & 0 & 0 & \frac{1}{2} & 0 & 0 \\ 0 & 0 & 0 & 0 & \frac{1}{2} & 0 \\ 0 & 0 & 0 & 0 & 0 & \frac{1}{2} \end{bmatrix} \tag{8}$$

From comparison between Equations 5 and 8, it can be seen that leading diagonal elements of Equation 5 are definitely less than the corresponding elements in the elastic matrix $[D^e]$. This represents the reduction in the stiffness of the material element due to yielding. In addition, components of the shear strain- (or stress-) increments in Equation 5 are associated with components of normal stress- (or strain-) increments, and so some cross-effects in stress-strain relation are observed in the plastic range.

As a special case, the stress- and strain-increments in Equation 4 would be for the axisymmetric problems

$$\{d\sigma\} = \begin{Bmatrix} d\sigma_r \\ d\sigma_\theta \\ d\sigma_z \\ d\tau_{rz} \end{Bmatrix} \qquad \{d\epsilon\} = \begin{Bmatrix} d\epsilon_r \\ d\epsilon_\theta \\ d\epsilon_z \\ d\gamma_{rz} \end{Bmatrix} \tag{9}$$

The expression for $[D^p]$ in the axisymmetric case would be obvious, and not be necessary to describe here. The stress-strain matrix for plane strain problems is also simple and is expressed specifically for the case where $d\epsilon_z = 0$ ($d\gamma_{yz} = d\gamma_{zx} = 0$)

$$\begin{Bmatrix} d\sigma_x \\ d\sigma_y \\ d\tau_{xy} \end{Bmatrix} = \frac{E}{1+\nu} \begin{bmatrix} \frac{1-\nu}{1-2\nu} - \frac{\sigma_x'^2}{S} & & \text{SYM.} \\ \frac{\nu}{1-2\nu} - \frac{\sigma_x' \sigma_y'}{S} & \frac{1-\nu}{1-2\nu} - \frac{\sigma_y'^2}{S} & \\ -\frac{\sigma_x' \tau_{xy}}{S} & -\frac{\sigma_y' \tau_{xy}}{S} & \frac{1}{2} - \frac{\tau_{xy}^2}{S} \end{bmatrix} \begin{Bmatrix} d\epsilon_x \\ d\epsilon_y \\ d\gamma_{xy} \end{Bmatrix} \quad (10)$$

Equation 10 can be obtained by deleting the rows of $d\sigma_z$, $d\tau_{yz} = d\tau_{zx} = 0$ as well as the columns corresponding to $d\epsilon_z = d\gamma_{yz} = d\gamma_{zx} = 0$ in the plastic stress-strain matrix $[D^p]$ of Equation 5. As an additional special case, the following stress-strain matrix should be used in the case of Saint-Venant torsion problems to be discussed in Section IV

$$\begin{Bmatrix} d\tau_{yz} \\ d\tau_{zx} \end{Bmatrix} = 2G \begin{bmatrix} \frac{1}{2} - \frac{\tau_{yz}^2}{S} & -\frac{\tau_{yz} \tau_{zx}}{S} \\ -\frac{\tau_{yz} \tau_{zx}}{S} & \frac{1}{2} - \frac{\tau_{zx}^2}{S} \end{bmatrix} \begin{Bmatrix} d\gamma_{yz} \\ d\gamma_{zx} \end{Bmatrix} \quad (11)$$

where z axis is taken along the centroidal axis of a bar.

The stress-strain matrix for plane stress problems ($\sigma_z = 0$) can be obtained by putting $d\sigma_z = 0$ in Equation 4 and eliminating the corresponding strain component $d\epsilon_z$ therefrom. However, the authors have found that it is simpler to derive it directly by using the original Equations 1 and 7. Putting $\sigma_z = 0$ in Equation 1 and retaining the necessary equations and/or terms, we obtain

$$\begin{aligned} d\epsilon_x &= \sigma_x' \, d\lambda + \frac{1}{E} (d\sigma_x - \nu \, d\sigma_y) \\ d\epsilon_y &= \sigma_y' \, d\lambda + \frac{1}{E} (d\sigma_y - \nu \, d\sigma_x) \\ d\gamma_{xy} &= 2\tau_{xy} \, d\lambda + 2 \frac{1+\nu}{E} \, d\tau_{xy} \end{aligned} \quad (12)$$

and

$$d\lambda = \frac{9}{4} \frac{\sigma_x' \, d\sigma_x + \sigma_y' \, d\sigma_y + 2\tau_{xy} \, d\tau_{xy}}{\bar{\sigma}^2 H'} \quad (13)$$

Substituting $d\lambda$ from Equation 13 into 12 and solving for the stress-increments

$$\begin{Bmatrix} d\sigma_x \\ d\sigma_y \\ d\tau_{xy} \end{Bmatrix} = \frac{E}{Q} \begin{bmatrix} \sigma_y'^2 + 2P & & \text{SYM.} \\ -\sigma_x'\sigma_y' + 2\nu P & \sigma_x'^2 + 2P & \\ -\frac{\sigma_x' + \nu\sigma_y'}{1+\nu}\tau_{xy} & -\frac{\sigma_y' + \nu\sigma_x'}{1+\nu}\tau_{xy} & \frac{R}{2(1+\nu)} + \frac{2H'}{9E}(1-\nu)\bar{\sigma}^2 \end{bmatrix} \begin{Bmatrix} d\epsilon_x \\ d\epsilon_y \\ d\gamma_{xy} \end{Bmatrix} \quad (14)$$

where

$$P = \frac{2H'}{9E}\bar{\sigma}^2 + \frac{\tau_{xy}^2}{1+\nu}, \qquad Q = R + 2(1-\nu^2)P$$
$$R = \sigma_x'^2 + 2\nu\sigma_x'\sigma_y' + \sigma_y'^2 \quad (15)$$

Using Equation 14, we can represent the stress-increments in Equation 13 in terms of strain-increments, and obtain an alternative expression for $d\lambda$

$$d\lambda = \frac{1}{Q}\left[(\sigma_x' + \nu\sigma_y')\, d\epsilon_x + (\sigma_y' + \nu\sigma_x')\, d\epsilon_y + (1-\nu)\tau_{xy}\, d\gamma_{xy}\right] \quad (16)$$

The proportionality factor $d\lambda$ or the corresponding plastic equivalent strain-increment $\overline{d\epsilon}^P = 2\bar{\sigma}\, d\lambda/3$ should be positive for continued loadings. In the case of the strain-hardening materials, this check of sign can be made by using Equations 7 and 13. But for the nonhardening materials with $H' = 0$ the check should be made by Equations 2 and 16. Since it is easily proved that Q involved in Equation 16 is positive, the sign of $d\lambda$ for plane stress problems can be checked only by examination of the term in the square bracket of Equation 16.

SECTION III

APPLICATION FOR THE SOLUTION OF CONTINUUM PROBLEMS AND SOME NUMERICAL EXAMPLES

Using the plastic stress-strain matrix obtained in the preceding section, the characteristic stiffness of the individual finite element in the plastic state can be evaluated. In the case of the plane stress field, for example, the stiffness matrix $\left[k^P\right]$ of a triangular element can be expressed as

$$\left[k^P \right] = \left[N \right]^T \left[D^P \right] \left[N \right] t \Delta \tag{17}$$

where t denotes the plate thickness of the element which is assumed to be constant, and Δ is the area of a given triangle. The matrix $\left[N\right]$ is identical with $\left[B\right]$ defined by Equation (3.10) in Zienkiewicz (Reference 2). And $\left[N\right]^T$ is the transpose of the matrix $\left[N\right]$.

In the case of the axisymmetric problems (Figure 1), Equation 17 is to be replaced by

$$\left[k^P \right] = 2\pi \left[\bar{N} \right]^T \left[D^P \right] \left[\bar{N} \right] \bar{r} \Delta \tag{18}$$

in which Δ implies the area of a triangle as shown in Figure 1. Approximation of the mean radius $\bar{r}$ is used in Equation 18 as well as in the numerical examples to be shown later. $\left[\bar{N}\right]$ is again identical with $\left[\bar{B}\right]$ defined by Equation (4.14) in Zienkiewicz (Reference 2).

Procedure of assembling the overall or complete stiffness matrix of the whole body is the same as that in the corresponding elastic problems except using plastic stiffness matrix such as Equations 17 and 18 for the yielded elements. The stiffness matrix thus assembled represents the reduced stiffness at each stage of the expansion of the plastic region. However, so long as the plastic region does not develop to a large extent, i.e. in the case of the contained plastic problems, reduction of the overall stiffness may not be profound because of the restraint of the neighbors which continue to be in the elastic state. If the material is assumed to be nonhardening, the ultimate condition which corresponds to the 'limiting state' in the plastic or limit analysis will be automatically attained by continuous tracing of the whole solution in the elastic-plastic range.

The method of solution proposed by Yamada, Yoshimura, and Sakurai (Reference 7) employs the stress-strain and stiffness matrices so far described, and is purely incremental in that the load-increment just enough to cause yielding of a single discrete element is used

at each loading stage. Accordingly the load-increment is not a constant and is specified as the consequence of the calculation. Instead of reintroducing the details of the calculation procedures, the method of determination of the load-increment at each stage will be only described here.

In the case of the usual triangular element adopted for plane stress analysis, the stresses as well as strains are constant throughout the element. Similarly, in the approximate treatment of axisymmetric problems where the mean radius $\bar{r}$ and the mean value of z coordinate are used, we can assume the stresses and strains in each element to be constant. Under these circumstances, the yield condition of the triangular element is given by

$$\bar{\sigma} = \sqrt{\frac{3}{2}\,\sigma'_{ij}\;\sigma'_{ij}} = Y \tag{19}$$

where the Mises yield condition has been employed, and $\bar{\sigma}$, σ'_{ij} are the equivalent and the deviatoric stresses respectively. Y denotes the yield stress determined by the tensile or compression test. When $\bar{\sigma}$ in a certain element reaches Y, the element is regarded to be in plastic (or yielded) state.

Having obtained the solutions up to the jth stage of calculation, the subsequent stress-increment $\Delta\sigma_{ij}^{t}$ is calculated by carrying out the usual analysis with respect to the assumed test load $\{\Delta L^{t}\}$. By this process, the stress-increment PR of each elastic element from the known state of stress P at jth stage can be determined (Figure 2). Relation between the stress $\sigma_{ij} + \Delta\sigma_{ij}^{t}$ at R and the equivalent stress $\bar{\sigma} + \Delta\bar{\sigma}^{t}$ is given by the following equation:

$$\bar{\sigma} + \Delta\bar{\sigma}^{t} = \sqrt{\frac{3}{2}\left(\sigma'_{ij} + \Delta\sigma'^{t}_{ij}\right)\left(\sigma'_{ij} + \Delta\sigma'^{t}_{ij}\right)} \tag{20}$$

The stress-increment required to cause yielding of elastic element sould be given by PQ in Figure 2. Thus, denoting PQ/PR = r, we obtain

$$Y = \sqrt{\frac{3}{2}\left(\sigma'_{ij} + r\,\Delta\sigma'^{t}_{ij}\right)\left(\sigma'_{ij} + r\,\Delta\sigma'^{t}_{ij}\right)} \tag{21}$$

r can be determined from Equations 20 and 21

$$\left.\begin{aligned} r &= \frac{\Gamma + \left[\Gamma^2 + 4\left(\overline{\Delta\sigma_{ij}}^{t}\right)^2\left(Y^2 - \bar{\sigma}^2\right)\right]^{1/2}}{2\left(\overline{\Delta\sigma_{ij}}^{t}\right)^2} \\ \Gamma &= \left(\overline{\Delta\sigma_{ij}}^{t}\right)^2 - 2\bar{\sigma}\,\Delta\bar{\sigma}^{t} - \left(\Delta\bar{\sigma}^{t}\right)^2 \end{aligned}\right\} \tag{22}$$

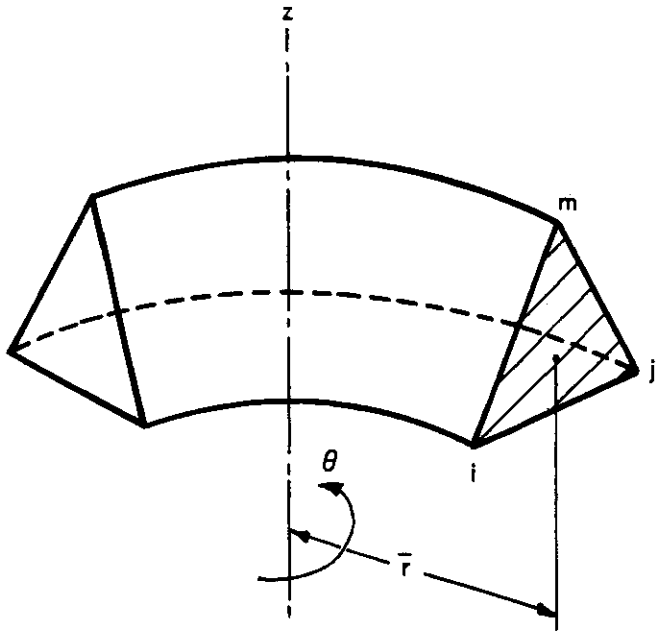

Figure 1. Triangular Element in Axisymmetric Problem

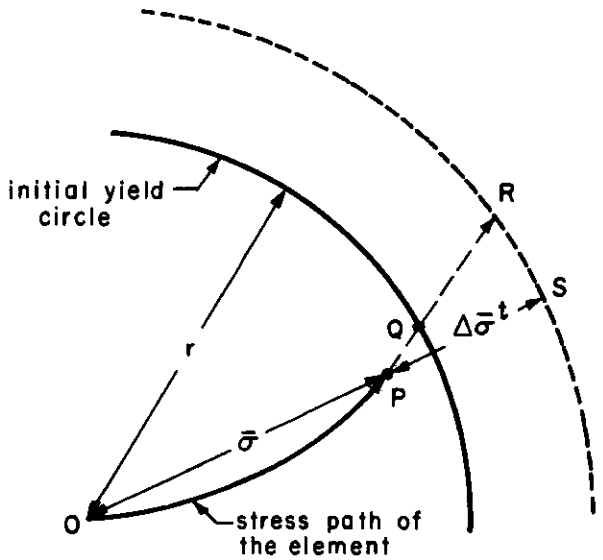

$$PR = \overline{\Delta\sigma}_{ij}^{t} \,, \quad r = PQ/PR$$

Figure 2. Determination of the Load Increment Just Enough to Cause Yielding of the Elastic Element

where

$$\overline{\Delta\sigma_{ij}}^{\,t} = \sqrt{\frac{3}{2}\,\Delta\sigma'^{t}_{ij}\;\;\Delta\sigma'^{t}_{ij}} = \text{PR of Figure 2}$$

$\Delta\bar{\sigma}^{t}$ involved in Equation 22 can be evaluated by subtracting $\bar{\sigma}$ at the preceding stage from $\bar{\sigma}+\Delta\bar{\sigma}^{t}$ calculated by Equation 20 for the assumed test load.

Following the procedures mentioned above, r can be found for all the elements which remain elastic at jth stage, and the minimum of which is designated by r_{min}. The element (or elements) having r_{min} is nearest to yielding at the relevant stage and can be regarded to be yielded in the next $(j+1)$ th load-increment which is $r_{min}\{\Delta L^{t}\}$. The specific form of (22) for Saint-Venant torsion problems to be discussed in the next section is

$$r = \frac{\Gamma + \left[\Gamma^{2} + 4\,(\overline{\Delta\tau}^{\,t})^{2}\,(k^{2}-\tau^{2})\right]^{1/2}}{2(\overline{\Delta\tau}^{\,t})^{2}} \tag{23}$$

where

$$\Gamma = (\overline{\Delta\tau}^{\,t})^{2} - 2\tau\,\Delta\tau^{t} - (\Delta\tau^{t})^{2}$$

$$\tau = \sqrt{\tau_{yz}^{2}+\tau_{zx}^{2}}\,,\quad \tau+\Delta\tau^{t} = \sqrt{(\tau_{yz}+\Delta\tau^{t}_{yz})^{2}+(\tau_{zx}+\Delta\tau^{t}_{zx})^{2}}$$

and

$$\overline{\Delta\tau}^{\,t} = \sqrt{(\Delta\tau^{t}_{yz})^{2}+(\Delta\tau^{t}_{zx})^{2}}$$

The first numerical examples worked out by the authors were the plane stress problems of 90 degree V-notched and slit-notched tension specimens (Reference 7). Here we present recent examples which concern with the plane and axisymmetric problems of 60 degree V-notched tension specimens with a small bottom notch radius in Figure 3 (Reference 8). Major difference between specimens with round bottom notches and with sharp ones is that the plastic zones surround the notch sides considerably in the former. It has been observed from comparison between plane stress and axisymmetric solutions that the development of the plastic zone is rapid in the former, that is the spread of the yielded region of the plate specimen is broader at the same level of nominal axial stress P/AY. In the examples shown in Figure 3, the materials have been assumed to work-harden obeying the stress-strain relation $\bar{\sigma} = 53+420\sqrt{\bar{\varepsilon}^{P}}$, and the change of shape due to large displacements or deformations of the elements has been taken into account.

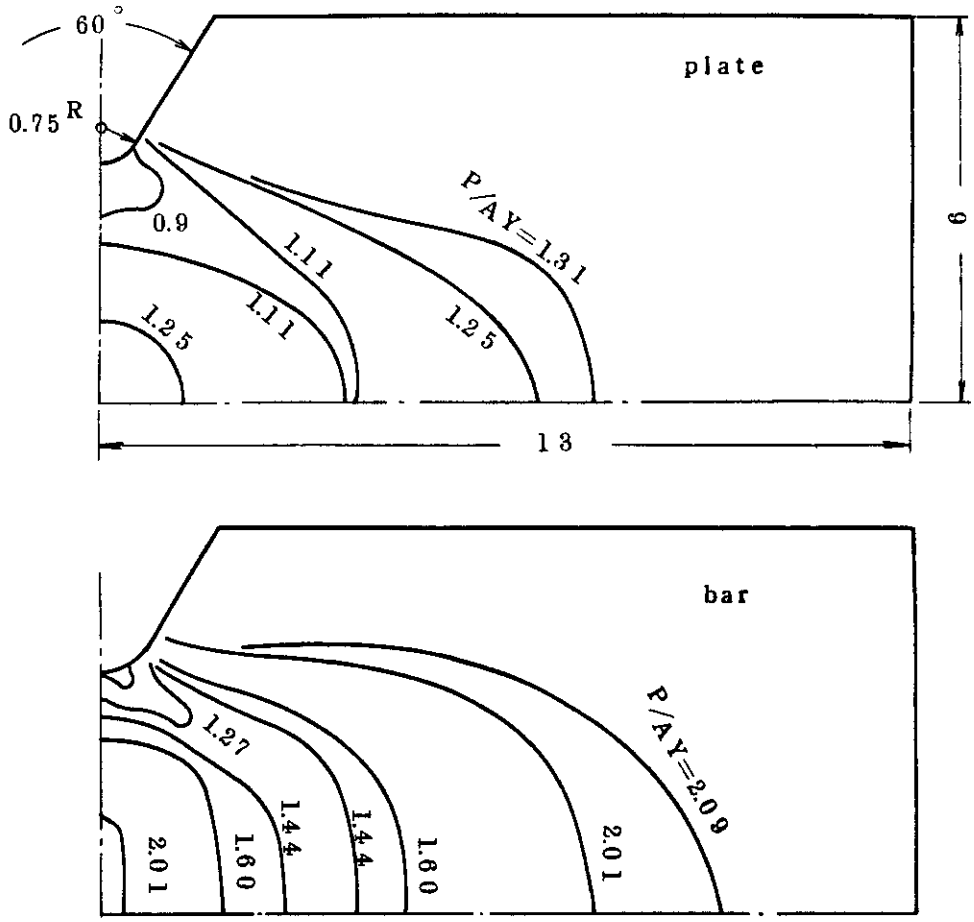

Figure 3. Sixty-degree V-notched Plate and Bar Specimens Under Tensile Test, Showing the Successive Expansion of Plastic Region in Quadrant

SECTION IV

SAINT-VENANT TORSION

General treatment of Saint-Venant torsion problems is relatively simple, and it provides a good example of the application of basic principles in continuum mechanics where it is possible to give physical interpretation to the principles. The finite element method as applied to the Saint-Venant torsion problems by means of the stress function has been well established (Reference 2). Using the prismatic element as shown in Figure 4 and denoting the stress function by ϕ, the expressions for shearing stresses τ_{yz} and τ_{zx} are as follows:

$$\tau_{yz} = -\frac{\partial \phi}{\partial x} = -\frac{1}{2A}\begin{bmatrix} b_i & b_j & b_m \end{bmatrix}\begin{Bmatrix} \phi_i \\ \phi_j \\ \phi_m \end{Bmatrix} \tag{24}$$

$$\tau_{zx} = \frac{\partial \phi}{\partial y} = \frac{1}{2A}\begin{bmatrix} C_i & C_j & C_m \end{bmatrix}\begin{Bmatrix} \phi_i \\ \phi_j \\ \phi_m \end{Bmatrix} \tag{25}$$

where

$$\left.\begin{aligned} b_i &= y_j - y_m, \quad b_j = y_m - y_i, \quad b_m = y_i - y_j \\ C_i &= x_m - x_j, \quad C_j = x_i - x_m, \quad C_m = x_j - x_i \end{aligned}\right\} \tag{26}$$

As usual, z axis is taken along the centroidal axis of a bar and x and y axes lie in the plane of a cross-section.

The equations for the determination of stress function ϕ are expressed as

$$\sum_i \sum_j h_{ij}\phi_j - \sum_i F_i = 0 \tag{27}$$

where $\sum_i$ implies summation over all the prismatic elements having their vertices of triangle at the nodal point i. The boundary condition for the solution of ϕ is along the contour of the cross section

$$\phi = \text{const.}$$

h_{ij} is the element of i th row and j th column of the matrix $[h]$ which is

$$[h] = \frac{1}{4A_i}\left[\{b_j\}[b_j] + \{c_j\}[c_j]\right], \quad j = i, j, m \tag{28}$$

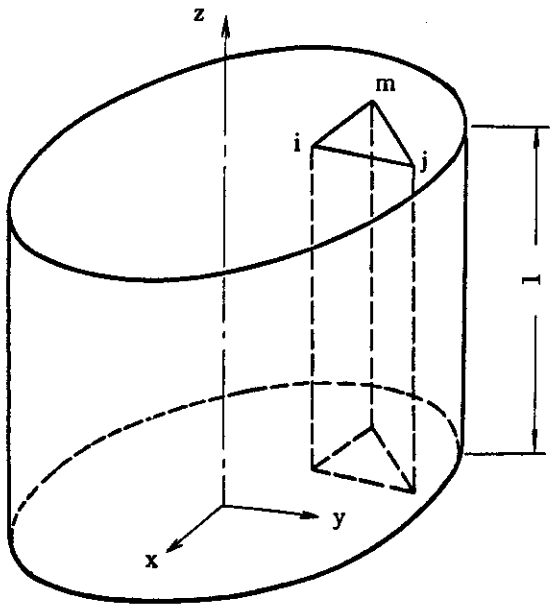

Figure 4. Prismatic Element as Used for the Analysis of Saint-Venant Torsion Problems

and F_i denotes

$$F_i = \frac{2}{3} G \theta A_i \tag{29}$$

where A_i refers to the cross-sectional area of the relevant prism. G is the shear modulus and θ is the angle of twist per unit length along the bar. Using Equations 24 and 25, we can write Equation 27 in an alternative form as

$$-\frac{1}{2} \sum_i b_i (\tau_{yz})_i + \frac{1}{2} \sum_i C_i (\tau_{zx})_i - \sum_i \frac{2}{3} G \theta A_i = 0 \tag{30}$$

where $(\tau_{yz})_i$ and $(\tau_{zx})_i$ are the shearing stresses in the prismatic elements which meet at the nodal point i ; these stresses being constant throughout each element in the framework of the theory.

It should be noted here that Equation 30 is equivalent to the following relation:

$$\oint \tau_i \, d\bar{S} - 2G\theta \sum_i \bar{A}_i = G \oint dw = 0 \tag{31}$$

where $d\bar{S}$ represents a line element passing through the centroid of triangle and parallel to the edge opposite to the nodal point i (Figure 5) and $\bar{A}_i = 4A_i/9$. τ_i is the shearing stress along $d\bar{S}$, and w denotes the warping function. Equation 31 implies that the line integral of the warping function along the closed path is zero, i. e. the warping function is single-valued.

It is known, in general, that the approximate compatibility equations can be derived from the principle of the minimum complementary energy. (Reference 9) The above discussion exemplifies the application of the principle and makes clear the physical meaning of the finite element method based on the stress function.

Contrasting to the method by means of the stress function (which belongs to the force method), Kawai and Yoshimur (Reference 10) have proposed a method which keeps the warping function as variable and essentially is one of the displacement method. Their method uses the following well-known displacement function:

$$u = -\theta yz \quad , \quad v = \theta xz \quad , \quad w = w(x, y) \tag{32}$$

where u, v and w are displacement components along x, y and z axes respectively. In the method, the bar of uniform cross section is again divided into the prismatic elements, and the warping function w of Equation 32 is assumed to be represented, in each discrete element, by the linear function

$$w = \alpha_1 + \alpha_2 x + \alpha_3 y \tag{33}$$

Denoting the angle of twist, the values of warping at nodal points i, j, m of an element by θ, w_i, w_j and w_m, the moment M corresponding to θ and the nodal force vector $(Z_i \quad Z_j \quad Z_m)$ can be shown to be expressed as

$$\begin{Bmatrix} M \\ Z_i \\ Z_j \\ z_m \end{Bmatrix} = \iint \left[N\right]^T \left[D^e\right] \left[N\right] dx\, dy \begin{Bmatrix} \theta \\ w_i \\ w_j \\ w_m \end{Bmatrix} \tag{34}$$

where

$$\left[N\right] = \frac{1}{2A} \begin{bmatrix} -2Ay & b_i & b_j & b_m \\ 2Ax & c_i & c_j & c_m \end{bmatrix} \tag{35}$$

and

$$\left[D^e\right] = G \begin{bmatrix} 1 & 0 \\ 0 & 1 \end{bmatrix} \tag{36}$$

$\left[N\right]^T$ is the transpose of $\left[N\right]$ and $b_1, \ldots, c_i, \ldots$ are given by Equation 26 and A is the cross-sectional area of the prism as before.

The shearing stresses τ_{yz} and τ_{zx} in the element can be shown to be given as

$$\begin{Bmatrix} \tau_{zx} \\ \tau_{yz} \end{Bmatrix} = \left[D^e \right] \left[N \right] \begin{Bmatrix} \theta \\ w_i \\ w_j \\ w_m \end{Bmatrix} \tag{37}$$

Therefore M in Equation 34 is

$$M = \iint (x\tau_{yz} - y\tau_{zx}) \, dx \, dy$$

and it represents the twisting moment which each element will carry. Denoting the mean shearing stresses in the element by $(\tau_{zx})_{mean}$ and $(\tau_{yz})_{mean}$, the following relation will result

$$\begin{Bmatrix} Z_i \\ Z_j \\ Z_m \end{Bmatrix} = \frac{1}{2} \begin{bmatrix} b_i & c_i \\ b_j & c_j \\ b_m & c_m \end{bmatrix} \begin{Bmatrix} (\tau_{zx})_{mean} \\ (\tau_{yz})_{mean} \end{Bmatrix} \tag{38}$$

Thus as indicated in Figure 6, it can be seen that Z_i is equal to one-half of the resultant shearing force acting on the edge surface (whose area is $jm \times 1$) opposite to the nodal point i. And so, summing up the shearing forces in z direction of the prismatic elements which meet at the nodal point i in usual way and equating it to zero, the approximate force equilibrium condition in z direction can be obtained. This result coincides with the Veubeke's discussion (Reference 11) on the plane stress problems.

In order to compare the elastic solutions by the two methods above, torsion of a bar with elliptic section as shown in Figure 7 has been studied. Assuming in arbitrary unit $M=4$, $G=10^6$, $a=2$ and $b=1$, results obtained by the two different methods are given in Table 1 together with the exact solution. Comparison is made for shearing stresses at five points A, B, C, D, and E of Figure 7 and the angle of twist θ associated with the input data. From the results shown, it can be concluded that the accuracy of the displacement method is satisfactory. Further improvement would be expected by considering the implication of the approximate equilibrium condition indicated referring to Figure 6, and making reasonable division of the cross section in the neighborhood of the boundary.

The matrix displacement method so far developed for the solution of the elastic Saint-Venant torsion problems can be extended to elastic-plastic range by applying the

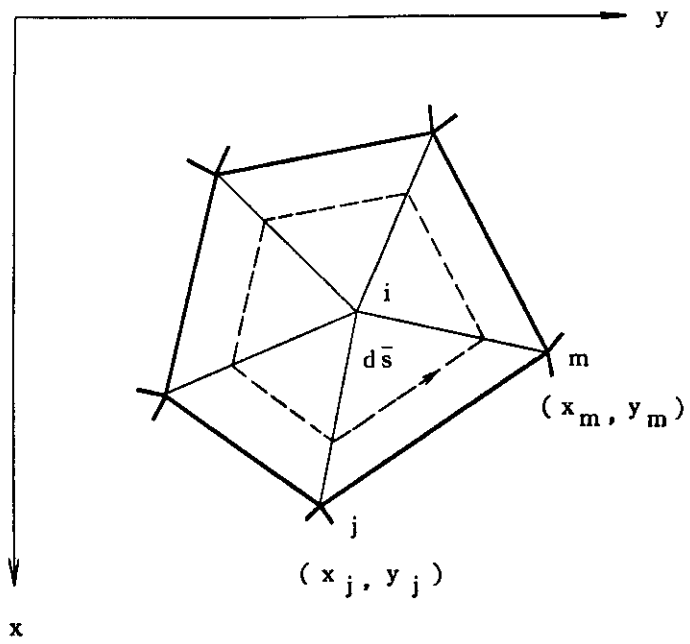

Figure 5. Closed Path Around the Nodal Point i

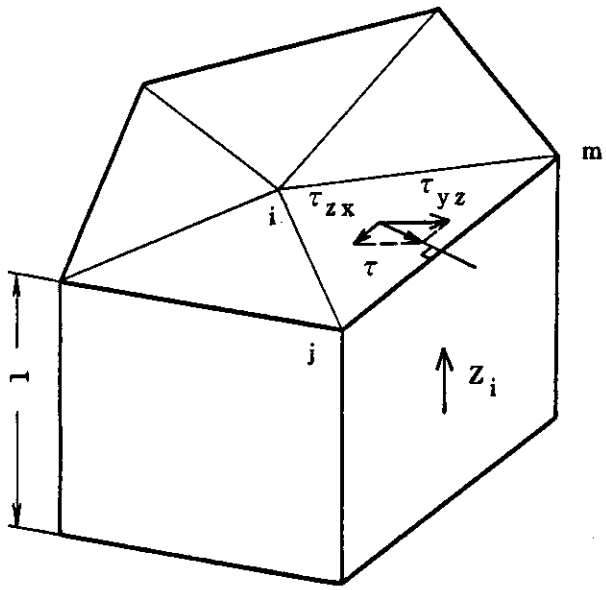

Figure 6. Prismatic Elements Meeting at the Nodal Point i and Shearing Forces

TABLE 1. COMPARISON OF THE NUMERICAL RESULTS, TORSION OF A BAR OF ELLIPTIC SECTION

(a) exact solution (b) force method (c) present displacement method

		A	B	C	D	E
τ_{yz}	(a)	1.27324	0.	1.26686	0.90928	0.50930
	(b)	1.231	0.	1.2245	0.9056	0.5086
	(c)	1.27135	0.	1.24450	0.90474	0.50926
τ_{zx}	(a)	0.	-0.63662	-0.06366	-0.44563	-0.19099
	(b)	0.	-0.6257	-0.06173	-0.44845	-0.19340
	(c)	0.	-0.64781	-0.06471	-0.44861	-0.19226
θ (rad.)		(a) 0.795775×10^{-6}	(b) 0.805000×10^{-6}	(c) 0.796953×10^{-6}		

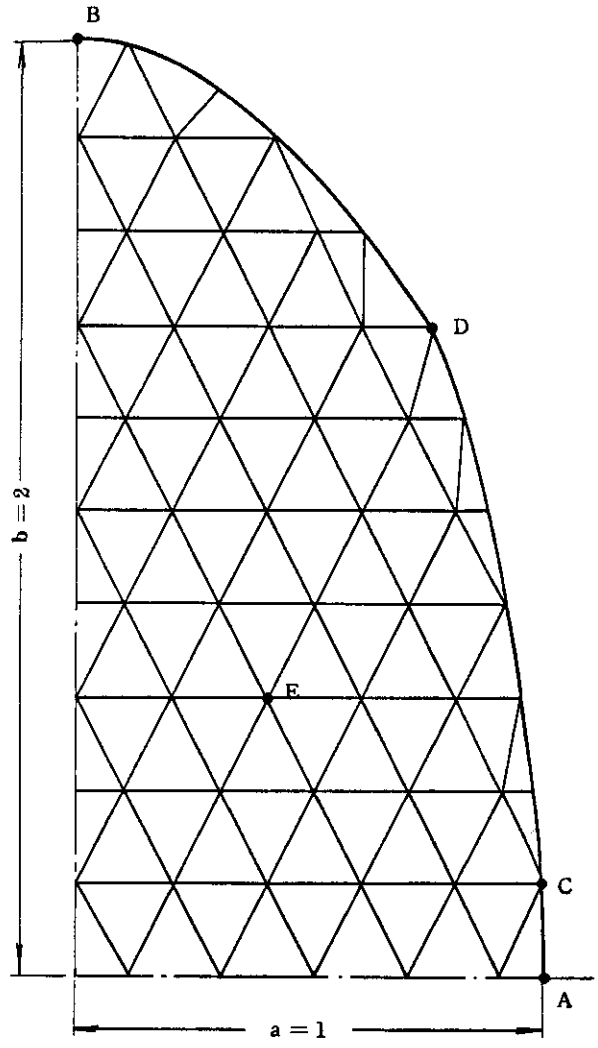

Figure 7. Torsion of a Bar of Elliptic Section, Showing the Division of the Section as Used in the Calculations.

procedure discussed in Section III. More precisely, in place of $[D^e]$ defined by Equation 36, Equation 11 should be adopted with

$$\left.\begin{aligned} S &= \frac{2}{3}\,\bar{\sigma}^2\left(1+\frac{H'}{3G}\right) = 2\tau^2\left(1+\frac{d\tau/d\gamma^P}{G}\right) \\ \tau &= \sqrt{\tau_{yz}^2+\tau_{zx}^2} \end{aligned}\right\} \tag{39}$$

$d\tau/d\gamma^P$ is the slope of the shearing stress-plastic strain curve determined by torsional testing of the thin-walled circular tube. The condition whether a specific element is yielded or not may be checked by using Equation 23.

In contrast to the treatment of the work-hardening material, the Saint-Venant torsion problems of the non-hardening material may need a somewhat different consideration. It is known that the shearing stress τ in the yielded element remains constant both in magnitude and direction once the element has become plastic and therefore the following relation holds (Reference 1).

$$d\gamma_{yz}\,/\,d\gamma_{zx} = \tau_{yz}\,/\,\tau_{zx} \tag{40}$$

Substituting this into Equation 11 and using Equation 39 with $d\tau/d\gamma^P = 0$ for the non-hardening material, the condition of constancy of τ (i.e. $d\tau_{yz} = d\tau_{zx} = 0$ would be confirmed.

It follows, for the yielded elements of the nonhardening material

$$\{P\} = \begin{Bmatrix} M \\ Z_i \\ Z_j \\ Z_m \end{Bmatrix} = \iint [N]^T \begin{Bmatrix} \tau_{zx}^e \\ \tau_{yz}^e \end{Bmatrix} dx\,dy \tag{41}$$

where τ_{zx}^e, τ_{yz}^e represent the shearing stresses at onset of yielding of the relevant element. Using Equation 34 for the elastic elements and Equation 41 for the yielded elements which have their nodal points on the elastic-plastic boundary, the force equilibrium equations at nodal points in the elastic region (including the nodal points on the elastic-plastic boundary) will be formulated. These equations determine the warping function in the elastic region and in particular on the elastic-plastic boundary. And afterwards, the warping in the plastic region can be calculated, if necessary. Equation 37 is still valid for the stresses in the elastic region. If the differential forms of Equation 34 and Equation 41 are used, the calculation procedures may be somewhat simplified. The differential forms are for the

elastic elements

$$\left\{ dP \right\} = \begin{Bmatrix} dM \\ dZ_i \\ dZ_j \\ dZ_m \end{Bmatrix} = \iint \left[N \right]^T \left[D^e \right] \left[N \right] dx\, dy \begin{Bmatrix} d\theta \\ dw_i \\ dw_j \\ dw_m \end{Bmatrix} \tag{42}$$

and for the post-yielded elements $\left\{ dP \right\} = 0$

As an alternative of the displacement method, the force method of solution (especially incremental approach) for the elastic-plastic torsion problems may be similarly formulated where the stress function will be employed again. However, it is the authors' opinion that the displacement method would be superior to the force method for Saint-Venant torsion problems because by the former (1) problems of multiple-connected region may be easily treated, (2) the warping as well as stress distributions can be readily determined with excellent accuracy such as shown in Table 1, and (3) from the viewpoints of structural engineering practice, automatic calculation of torsional properties (such as the warping-torsional rigidities, location of the shear center beside the Saint-Venant torsional stiffness) of structural shapes with complicated cross sections will be possible.

SECTION V

TRUSSES AND FRAME STRUCTURES

In the case of pin-jointed trusses, individual structural member can only carry axial forces. Therefore, in analyzing their elastic-plastic problems it is only necessary to replace the Young's modulus E by the tangent modulus $E_t = d\sigma/d\epsilon$ for the yielded members; σ and ϵ being axial stress and axial total strain respectively in the tensile or compression test of the member. Elastic-plastic analysis of trusses is entirely similar to that of the continua irrespective of the material property (i.e. strain-hardening or not), and since the number of structural members in trusses is finite, the solution to be obtained will be exact within the theory of structures.

In the elastic-plastic analysis of rigid frames, on the other hand, it is a common practice to adopt the concept of 'plastic hinge' and to assume the yielding of structural members at the positions of the maximum bending moment. Besides these, assumptions made by Livesley (Reference 12) in the collapse analysis will be employed in the following. Thus neglecting the effects of axial thrust on the bending moment, and adopting the notations of Livesley, the simplest load-displacement equations take the following form (Figure 8):

$$\left.\begin{aligned} P_1 &= K_{11}\, d_1 + K_{12}\, d_2 \\ P_2 &= K_{21}\, d_1 + K_{22}\, d_2 \end{aligned}\right\} \tag{43}$$

where

$$P_1 = \begin{Bmatrix} P_{x1} \\ P_{y1} \\ m_1 \end{Bmatrix} \qquad P_2 = \begin{Bmatrix} P_{x2} \\ P_{y2} \\ m_2 \end{Bmatrix} \qquad d_1 = \begin{Bmatrix} \delta_{x1} \\ \delta_{y1} \\ \theta_1 \end{Bmatrix} \qquad d_2 = \begin{Bmatrix} \delta_{x2} \\ \delta_{y2} \\ \theta_2 \end{Bmatrix}$$

and

$$K_{11} = \begin{bmatrix} EA/L & 0 & 0 \\ 0 & 12EI/L^3 & 6EI/L^2 \\ 0 & 6EI/L^2 & 4EI/L \end{bmatrix} \tag{44}$$

$$K_{12} = K_{21}^T = \begin{bmatrix} -EA/L & 0 & 0 \\ 0 & -12EI/L^3 & 6EI/L^2 \\ 0 & -6EI/L^2 & 2EI/L \end{bmatrix} \tag{45}$$

$$K_{22} = \begin{bmatrix} EA/L & 0 & 0 \\ 0 & 12EI/L^3 & -6EI/L^2 \\ 0 & -6EI/L^2 & 4EI/L \end{bmatrix} \tag{46}$$

If the plastic hinge is formed at the member end 1, we have

$$m_1 = \pm m_p = \frac{6EI}{L^2}\delta_{y1} + \frac{4EI}{L}\theta_1 - \frac{6EI}{L^2}\delta_{y2} + \frac{2EI}{L}\theta_2$$

where m_p denotes the fully plastic bending moment. Substituting θ_1 from this equation into Equation 43, we obtain

$$\left.\begin{aligned} P_1 &= K_{11}\, d_1 + K_{12}\, d_2 + m_p\, C_1 \\ P_2 &= K_{21}\, d_1 + K_{22}\, d_2 + m_p\, C_2 \end{aligned}\right\} \tag{47}$$

where

$$K_{11} = \begin{bmatrix} EA/L & 0 & 0 \\ 0 & 3EI/L^3 & 0 \\ 0 & 0 & 0 \end{bmatrix} \tag{48}$$

$$K_{12} = K_{21}^T = \begin{bmatrix} -EA/L & 0 & 0 \\ 0 & -3EI/L^3 & 3EI/L^2 \\ 0 & 0 & 0 \end{bmatrix} \tag{49}$$

$$K_{22} = \begin{bmatrix} EA/L & 0 & 0 \\ 0 & 3EI/L^3 & -3EI/L^2 \\ 0 & -3EI/L^2 & 3EI/L \end{bmatrix} \tag{50}$$

$$C_1 = \pm \begin{bmatrix} 0 \\ \frac{3}{2}/L \\ 1 \end{bmatrix} \qquad C_2 = \pm \begin{bmatrix} 0 \\ -\frac{3}{2}/L \\ \frac{1}{2} \end{bmatrix} \tag{51}$$

Similarly, if the plastic hinge is formed at the member end 2, K_{11} , . . . and C_1 , . . . in Equations 48 through 51 can be shown to be

$$K_{11} = \begin{bmatrix} EA/L & 0 & 0 \\ 0 & 3EI/L^3 & 3EI/L^2 \\ 0 & 3EI/L^2 & 3EI/L \end{bmatrix} \tag{52}$$

$$K_{12} = K_{21}^T = \begin{bmatrix} -EA/L & 0 & 0 \\ 0 & -3EI/L^3 & 0 \\ 0 & -3EI/L^2 & 0 \end{bmatrix} \tag{53}$$

$$K_{22} = \begin{bmatrix} EA/L & 0 & 0 \\ 0 & 3EI/L^3 & 0 \\ 0 & 0 & 0 \end{bmatrix} \tag{54}$$

$$C_1 = \pm \begin{bmatrix} 0 \\ \frac{3}{2}/L \\ \frac{1}{2} \end{bmatrix} \qquad C_2 = \pm \begin{bmatrix} 0 \\ -\frac{3}{2}/L \\ 1 \end{bmatrix} \tag{55}$$

And when plastic hinges are formed at both ends 1 and 2, the expressions should be

$$C_1 = \pm \begin{bmatrix} 0 \\ 0 \\ 1 \end{bmatrix} \qquad C_2 = \pm \begin{bmatrix} 0 \\ 0 \\ 1 \end{bmatrix} \tag{56}$$

and the flexural terms in $K_{11}, K_{12}, K_{21}, K_{22}$ are zero.

Thus, Livesley has suggested a method for the elastic-plastic analysis of frames where stiffness matrices of the members are to be modified depending upon hinge formation at their ends. According to his method, translations δ_x , δ_y of all the joints and the rotations θ at member ends where no hinge was formed are determined first from the assembled overall load-displacement equations. After these calculations, rotations at the member ends of hinge formation can be determined, if necessary. The rotations at the hinge may vary from one member to the other. Therefore discontinuities of rotation or slope may exist at the positions of hinge formation.

Summarizing the Livesley's method, the load-displacement equations of the complete structure formed from members of nonhardening material (m_p = constant) can be written as

$$\mathbf{P} - \mathbf{f}(m_p) = \mathbf{K}\mathbf{d}$$

where $\mathbf{P}$ indicates the applied joint loads, and $\mathbf{d}$ indicates the corresponding joint displacements. $\mathbf{f}$ is a linear function of m_p which is formed from the various terms $m_p C_1$, $m_p C_2$ etc. As stated before, the overall stiffness matrix $\mathbf{K}$ is modified whenever a new plastic hinge is formed, and the stage where $\mathbf{K}$ becomes singular corresponds to the limiting state where the frame may collapse into mechanism.

In another method of the elastic-plastic frame analysis, the discontinuities of rotation at the plastic hinge (which will be called hinge-rotations hereafter) are used as new variables. The method has been proposed by Jennings and Majid (Reference 13) and independently by Yamada (Reference 14). In their method, the elastic load-displacement Equation 43 for the individual member are modified after the hinge is formed at the end (or ends) to

$$\left.\begin{aligned} P_1 &= K_{11} d_1 + K_{12} d_2 + C_{11} \theta_1^* + C_{12} \theta_2^* \\ P_2 &= K_{21} d_1 + K_{22} d_2 + C_{21} \theta_1^* + C_{22} \theta_2^* \end{aligned}\right\} \tag{57}$$

where θ^* implies hinge rotation. The stiffness matrices K_{11}, K_{12}, K_{21} and K_{22} are identical with Equations 44 through 46 in the elastic range. $C_{11}, \ldots, C_{22}$ represent column vectors which consist of the last column of corresponding matrices $K_{11}, \ldots, K_{22}$. It must be emphasized that Equation 57 are only applied to the yielded members (i. e. members that have hinges at either end or both) and θ_1^*, θ_2^* represent discontinuities of rotation at the ends of such member (Figure 9).

Using Equation 43 for the elastic members and Equation 57 for the yielded ones we can assemble in usual way the overall load-displacement equations as follows:

$$\mathbf{P} - \Sigma \mathbf{C} \theta^* = \mathbf{K} \mathbf{d} \tag{58}$$

where $\mathbf{C}$ implies a column vector which are formed from C_{11}, C_{12} and so on appearing in Equations 57, and Σ represents summation with respect to hinges already developed. Inverting Equation 58

$$\mathbf{d} = \mathbf{K}^{-1} \left[\mathbf{P} - \Sigma \mathbf{C} \theta^* \right] \tag{59}$$

Since $\mathbf{K}$ in this method is identical with that of elastic analysis, the inversion of $\mathbf{K}$ will be necessary once for all.

Substituting $\mathbf{d}$ from Equation 59 into the expressions of bending moment at the member ends where plastic hinges are formed, we can obtain a set of linear simultaneous equations for the external load vector $\mathbf{P}$ and hinge-rotations θ^* at every stage of hinge formation.

The collapse of the frame can be identified by the condition that a matrix consisting of coefficients of θ^* in these equations becomes singular.

As an example of the method of solution which uses the hinge-rotations θ^* as variables, a portal frame shown in Figure 10 is analyzed. This is the one discussed in Neal (Reference 15). The results are shown in Table 2 and are completely identical with those in the Neal's book. In the example of Figure 10, the hinges are formed in a sequence of positions E, B, C and D.

Figure 11 is a similar example, except that the beam is subjected to the distributed load. Plastic hinges may be formed at some intermediate points along the length of the beam under distributed load in this case. This possibility should be taken into account in the evaluation of the fixed end forces and moments at joints A and B equivalent to the distributed loadings. More precisely, the fixed end forces and moments should be modified when a hinge (or hinges) is formed at some intermediate points. In the example of Figure 11, the hinges are formed in a sequence of E, B, D, and C; the detailed results being shown in Table 3.

Fortunately, in this example, the last plastic hinge was found to be formed at C under distributed load, and so no difficulties were experienced in the analysis. The positions x of the maximum bending moment in the beam which are effected by every hinge formation are given in the last row of Table 3. If a hinge (or hinges) is found to develop at an intermediate point under distributed load at the earlier stage of the elastic-plastic analysis, it may be unavoidable, in order to continue calculations, that the location of the hinge is approximately fixed and consequently the yield condition is violated to some degree in the neighborhood of the hinge.

Two methods of solution are discussed so far on the elastic-plastic problems of structural frames. The authors believe that the latter method which takes the hinge rotations as variables would be preferable, since (1) the effects of strain-hardening at the plastic hinge may be easily incorporated and (2) we need compute only once the inverse of the matrix ΔK which remains unchanged during the whole process (in this discussion, the effects of axial thrust on the bending moment is not considered).

TABLE 2. ELASTIC-PLASTIC ANALYSIS OF PORTAL FRAME OF FIGURE 10

hinge formation at	E	B	C	D
$H\ell/m_p$	2.424	2.567	2.957	3.0
m_D/m_p	-0.5152	-0.5821	-0.9126	-1.0
m_A/m_p	-0.0303	-0.0149	-0.0043	0
m_C/m_p	0.7273	0.7761	1.0	1.0
m_B/m_p	-0.9394	-1.0	-1.0	-1.0
m_E/m_p	1.0	1.0	1.0	1.0
$\theta_D^* EI/m_p\ell$	—	—	—	—
$\theta_A^* EI/m_p\ell$	—	—	—	—
$\theta_C^* EI/m_p\ell$	—	—	—	0.1667
$\theta_B^* EI/m_p\ell$	—	—	-0.2174	-0.3333
$\theta_E^* EI/m_p\ell$	—	-0.0299	-0.1300	-0.1667

TABLE 3. ELASTIC-PLASTIC ANALYSIS OF PORTAL FRAME OF FIGURE 11

hinge formation at	E	B	D	C
$H\ell/m_p$	2.424	2.567	3.059	3.328
m_D/m_p	-0.5152	-0.5821	-1.0	-1.0
m_A/m_p	-0.0303	-0.0149	0.0588	0.3270
m_C/m_p	0.4811	0.5182	0.7376	1.0
m_B/m_p	-0.9394	-1.0	-1.0	-1.0
m_E/m_p	1.0	1.0	1.0	1.0
$\theta_D^* EI/m_p\ell$	—	—	—	-0.3808
$\theta_A^* EI/m_p\ell$	—	—	—	—
$\theta_C^* EI/m_p\ell$	—	—	—	—
$\theta_B^* EI/m_p\ell$	—	—	-0.2745	-0.7673
$\theta_E^* EI/m_p\ell$	—	-0.0299	-0.1569	-0.4928
position x of (m_C)max	0.750ℓ	0.744ℓ	0.769ℓ	0.734ℓ

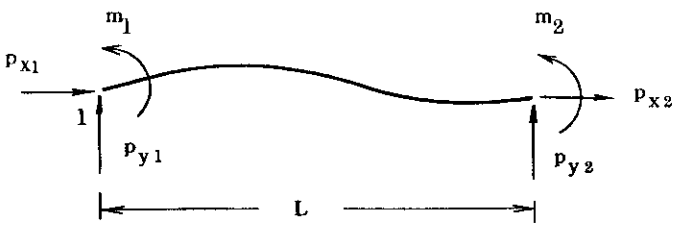

Figure 8. Notations for Loads in Plane Bending of a Uniform Member

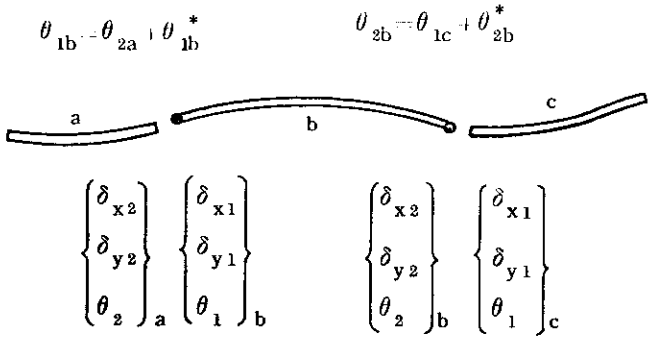

Figure 9. Plastic Hinge and Discontinuous Rotations

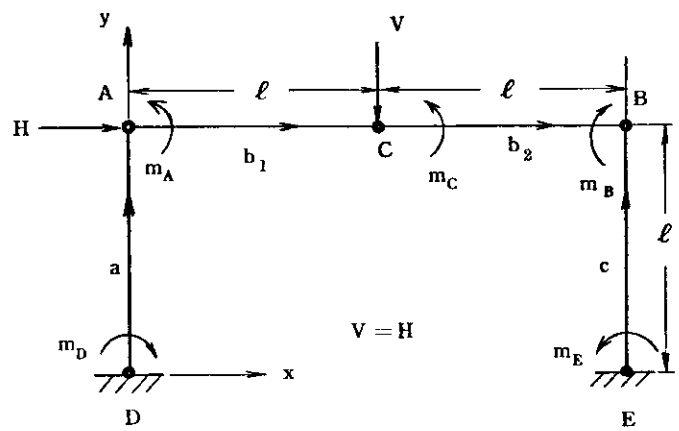

Figure 10. Simple Rectangular Portal Frame Subjected to Concentrated Loadings

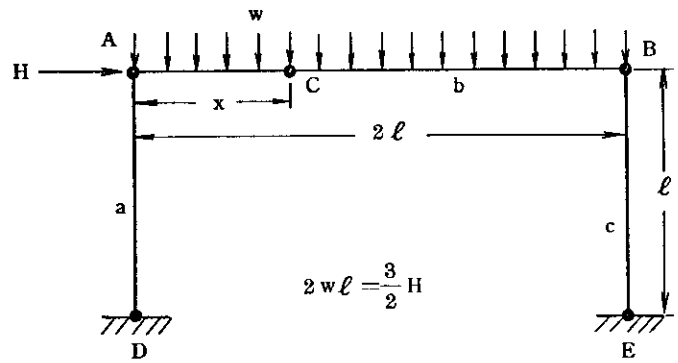

Figure 11. Portal Frame Under Distributed Loading Along the Length of the Beam

SECTION VI

REFERENCES

1. R. Hill, The Mathematical Theory of Plasticity. Clarendon Press, Oxford (1950).
2. O. C. Zienkiewicz, The Finite Element Method in Structural and Continuum Mechanics. McGraw-Hill, London and New York (1967).
3. G. G. Pope, Proc. "Conf. Matrix Methods in Structural Mechanics," p. 635. Air Force Inst. of Technology, Wright Patterson A. F. Base, Ohio (1965).
4. P. V. Marcal and W. R. Pilgrim, J. "Strain Analysis" 1, 339 (1966).
5. P. V. Marcal and I. P. King, Int. J. Mech. Sci. 9, 143 (1967).
6. Y. Yamada, "Seisan Kenkyu" 19, 75 (1967) (in Japanese).
7. Y. Yamada, N. Yoshimura and T. Sakurai, Int. J. Mech. Sci. 10. 343 (1968).
8. K. Setoguchi, unpublished data, Nagasaki Technical Institute, Mitsubishi Heavy Industries, Ltd.
9. K. Washizu, Variational Methods in Elasticity and Plasticity. Pergamon (1968).
10. T. Kawai and N. Yoshimura, "Seisan Kenkyu" 20, 246 (1968), (in Japanese).
11. F. de Veubeke, "Matrix Methods of Structural Analysis", AGARDograph 72, p. 165. Pergamon (1964).
12. R. K. Livesley, "Matrix Methods of Structural Analysis", p. 253. Pergamon and MacMillan (1964).
13. A. Jennings and K. Majid, "The Structural Engineer" 43, 407 (1965).
14. Y. Yamada, "Seisan Kenkyu" 20, 243 (1968), (in Japanese).
15. B. G. Neal, The Plastic Methods of Structural Analysis, p. 53. Chapman and Hall (1956).